

Second Harmonic and Fundamental Wavelengths Digital Holographic Microscopy

Etienne Shaffer*, Nicolas Pavillon, Jonas Kühn, and Christian Depeursinge

École Polytechnique Fédérale de Lausanne (EPFL), Advanced Photonics Laboratory, 1015
Lausanne Switzerland.

*Corresponding author: etienne.shaffer@epfl.ch

Abstract: We report on a new, multi-functional second harmonic generation digital holographic microscope that allows retrieval of an object complex diffraction wavefront at both second harmonic and fundamental wavelengths.

© 2009 Optical Society of America

OCIS codes: 090.1995 Digital Holography, 180.4315 Nonlinear Microscopy

1. Introduction

Digital holographic microscopy (DHM) is a full-field technique that allows real-time retrieval of the complex diffraction wavefront of an object. It can reveal deformations and morphological details at a nanometer-scale resolution [2], and determine with high precision the refractive index distribution across a sample [3] (e.g. cell); it is thus an excellent instrument for metrology and biological applications, especially since it is a non-intrusive, non-destructive imaging technique.

On the other hand, second harmonic generation (SHG), just like two-photons excitation fluorescence (TPEF), is a second order non-linear optical phenomenon that depends quadratically on the incident light intensity. However, SHG differs from TPEF in that it is an energy-conservative, coherent process. This means that SHG is potentially bleaching-free, in opposition to fluorescence, and that it is suitable for interferometric imaging techniques. In addition, since many cellular structures, rubulins or membranes generate second harmonic [5], labelling is not required. Among cutting-edge applications is monitoring of neuron membrane potentials by second harmonic generation (SHG) [6]. But despite the great potential of SHG, only Pu *et al.* [7] have yet reported work on harmonic holography imaging. In the framework of their ultrafast four-dimensional contrast microscopy, they presented second harmonic intensity contrast images of relatively large clusters (tens of micrometers) of $BaTiO_3$ nanoparticles.

In this work, we propose to combine SHG with DHM, and report on a microscope capable of taking amplitude and phase contrast images at both second harmonic and fundamental wavelengths.

2. Method

In digital holography, interference patterns (holograms) are recorded by a digital camera. In opposition to classical holography, no photo-chemical development step is required, and the image reconstruction is performed numerically.

In our configuration, the detector is located at a distance d from the system image plane and the intensity I_H recorded at the hologram plane is the resulting interference of the object wave O , and one reference wave R and can be expressed as:

$$I_H(x, y) = OO^* + RR^* + OR^* + R^*O \quad (1)$$

where the first two terms form a zero-order of diffraction and the last two respectively correspond to the real and the virtual images. The star symbol (*) denotes the complex conjugate. Since we work in an off-axis configuration, spatial frequency Fourier filtering allows to recover the desired image term. In this work we have had O and R both at fundamental, and successively frequency-doubled wavelengths. After Fourier filtering, the complex wave is numerically propagated to the image plane, at a distance d from the hologram plane, by means of a single Fresnel propagation, as explained in details in Ref. [10].

One major advantage with DHM is that any optical aberrations can be compensated by direct application of infinitely thin numerical parametric lenses to the complex wavefront, either or both in the hologram plane and/or the image plane. Information on numerical parametric lenses and automatic procedures developed for their application can be found in Ref. [1].

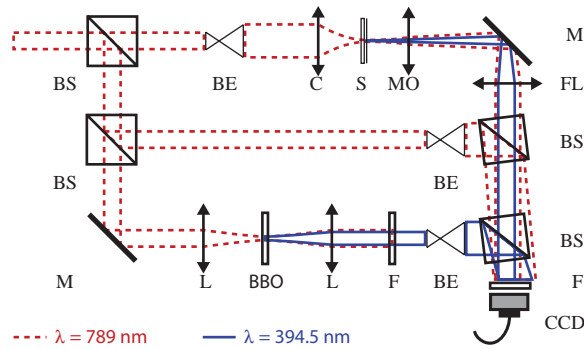


Fig. 1: Experimental setup schematics: *BS* beamsplitter, *C* condenser lens, *S* specimen, *MO* microscope objective, *M* mirror, *FL* field lens, *F* wavelength-selective filter, *BE* beam expander with pinhole-based spatial filtering, *L* lens, *BBO* frequency doubler β -barium borate crystal and *CCD* digital detector. Laser source is a 250-femtosecond Ti:Sapphire laser.

3. Experimental Details

Schematics of the experimental setup can be found in Fig. 1. Light source is a femtosecond laser equipped with a regenerative amplifier stage that delivers $5 \mu\text{J}$, 250 fs pulses at a repetition rate of approximately 250 kHz. The interferometer consists of one object arm containing the specimen and two reference arms for the fundamental and the frequency-doubled reference waves. In the object arm, light is focalized in the specimen plane to a spot size of about $30 \mu\text{m}$ and collected by a 100x, 1.3 NA oil immersion microscope objective, therefore allowing full-field imaging. The only noticeable difference between the two reference arms is the frequency doubler β -barium borate crystal inserted in the second reference arm to generate the second harmonic reference wave. Holograms were recorded using a -20°C -cooled *Hamamatsu Orca-ER* CCD camera. A ND5 neutral density filter and a $400 \pm 20 \text{ nm}$ bandpass filter were used for recording holograms at fundamental and second harmonic wavelengths, respectively.

The investigated specimen for the experiments described in this paper was a solution of 750nm-diameter polystyrene microspheres and 150nm-diameter BaTiO_3 nanoparticles, let to dry on a microscope slide and then covered with a $170 \mu\text{m}$ -thick glass cover slip. We show that second harmonic is material-selective and allows high-contrast discrimination between the two types of particles.

4. Results and Discussion

Reconstructed amplitude and phase contrast images reported in Fig. 2 present four relatively large polystyrene microspheres and a much smaller BaTiO_3 nanoparticle. Polystyrene microspheres do not generate detectable second harmonic at the laser fluence used for this experiment and can therefore only be seen in the fundamental wavelength images, in which the BaTiO_3 nanoparticle is barely distinguishable, due to its very small size. However, the latter becomes strikingly evident in the reconstructed second harmonic images, where it dominates over the very low background of second harmonic generated at the cover slip interfaces. This weak cover slip signal has an almost-constant phase that serves to reference the SHG phase from the object. It is conceivable that an in-line technique similar to that proposed here could be based on the interference between this slowly varying SHG wave and those produced by the specimen.

Digital focusing is one of many advantages of DHM. No only does it lift any constraints on the camera position relative to the system image plane, but it also becomes an essential feature to compensate for chromatic aberration, when working with two or more different wavelengths, as is the case for SHG DHM. While digital focusing of reconstructed images in fundamental wavelength can seem pretty intuitive, the matter is a bit more subtle for the second harmonic reconstruction of a few point-like sources. Furthermore, chromatic aberrations prevent from using exactly the same reconstruction distance as with fundamental wavelength, although this gives a very good first approximation to which finer adjustment can be provided by a method similar to the one used in confocal microscopy [11], i.e. simply by selecting the reconstruction distance that gives the highest intensity. This is illustrated in Fig. 3 that shows the intensity for different reconstruction distances along a linear profile.

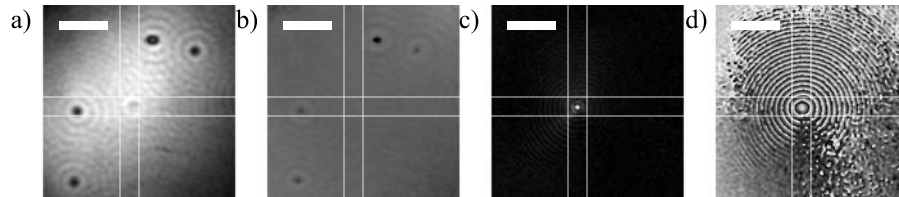


Fig. 2: Reconstructed in-focus amplitude (a, c) and phase (b, d) contrast images at fundamental (a, b) and second harmonic (c, d) wavelengths. 750 nm polystyrene microspheres are only visible in fundamental wavelength, while 150nm-diameter $BaTiO_3$ nanoparticle, barely distinguishable in fundamental wavelength generates strong second harmonic signal. Pale gray lines are guides and scale bars represent 5 microns.

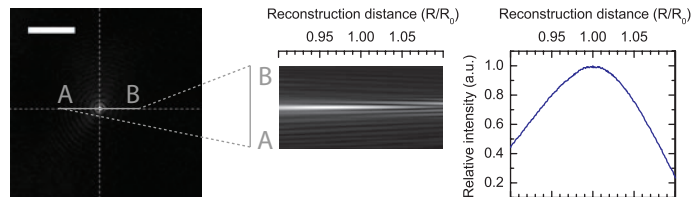


Fig. 3: Intensity (right) for different reconstruction distances along the profile AB (center) shown in the second harmonic generation amplitude image (left). Distances are expressed relatively to the optimal distance R_0 that brings the image in focus.

5. Conclusion

We have demonstrated that, thanks to its coherent nature, second harmonic generation is suitable for digital holographic microscopy. We have successfully recorded holograms in both fundamental and second harmonic wavelengths, extracted the complex field and numerically propagated it to reconstruct in-focus amplitude and phase contrast images, which is unprecedented. As expected, second harmonic provides high contrast, specific information, complementary to that obtained by classical DHM, which makes the proposed technique especially promising for material tagging and functional imaging. In addition, by granting access to the complex SHG emission wavefront, the technique can allow relative 3D positioning of nanoparticles in space. Finally, other, unpublished experiments we have carried out show that colloidal gold nanoparticles are also especially suitable for second harmonic generation. This leads us to believe that SHG DHM could become a tool of predilection for bio-conjugated agent tracking and high contrast imaging.

The authors would like to thank the EPFL STI Seed Fund for its financial support, as well as all members of the EPFL Microvision and Microdiagnostic Group, more specially Jérôme Parent and Dr Yves Delacrétaz for their technical assistance and fruitful discussions.

References

1. T. Colomb, F. Montfort, J. Kühn, N. Aspert, E. Cucho, A. Marian, F. Charrière, S. Bourquin, P. Marquet, and C. Depeursinge, *J. Opt. Soc. Am. A* **23**, 3177 (2006).
2. J. Kühn, F. Charrière, T. Colomb, E. Cucho, F. Montfort, Y. Emery, P. Marquet, and C. Depeursinge, *Meas. Sci. Technol.* **19**, 1 (2008).
3. P. Marquet, B. Rappaz, P. J. Magistretti, E. Cucho, Y. Emery, T. Colomb, and C. Depeursinge, *Opt. Lett.* **30**, 468 (2005).
4. F. Charrière, A. Marian, F. Montfort, J. Kühn, T. Colomb, E. Cucho, P. Marquet, and C. Depeursinge, *Opt. Lett.* **31**, 178 (2006).
5. W. R. Zipfel, R. M. Williams, R. Christie, A. Y. Nikitin, B. T. Hyman, and W. W. Webb, *Proc. Natl. Acad. Sci. USA* **100**, 7075 (2003).
6. D. A. Dombek, M. Blanchard-Desce, and W. W. Webb, *J. Neurosci.* **24**, 999 (2004).
7. Y. Pu, M. Centurion, and D. Psaltis, *Appl. Opt.* **47**, A103 (2008).
8. M. A. Hayat, *Colloidal Au: Principles, Methods and Applications* (Academic Press, 1989).
9. E. Cucho, P. Marquet, and C. Depeursinge, *Appl. Opt.* **39**, 4070 (2000).
10. U. Schnars and W. P. O. Juptner, *Meas. Sci. Technol.* **13**, R85 (2002).
11. C. J. R. Sheppard and H. J. Matthews, *J. Mod. Opt.* **35**, 145 (1988).